## ORDER, DISORDER, AND PHASE TRANSITION IN CONDENSED SYSTEMS

# Ab Initio Calculation of the Ferroelectric Phase Transition in Disordered and Ordered $PbSc_{0.5}Ta_{0.5}O_3$ and $PbSc_{0.5}Nd_{0.5}O_3$ Solid Solutions with the Use of a Model Hamiltonian

## V. I. Zinenko* and N. G. Zamkova**

*Kirensky Institute of Physics, Siberian Branch, Russian Academy of Sciences, Akademgorodok, Krasnoyarsk, 660036 Russia*
*\*e-mail: zvi@iph.krasn.ru*
*\*\*e-mail: zam@iph.krasn.ru*
Received July 2, 2007

**Abstract**—To describe the ferroelectric phase transition in ordered and disordered $PbSc_{0.5}Ta_{0.5}O_3$ (PST) and $PbSc_{0.5}Nd_{0.5}O_3$ (PSN) solid solutions, a model Hamiltonian is written in the local-mode approximation, in which long-range dipole–dipole and short-range interactions of local modes are taken into account. The Hamiltonian parameters are determined from the set of energies of a series of distorted structures, calculated within the nonempirical generalized Gordon–Kim model. The statistical mechanics of the systems with a model Hamiltonian is investigated by the Monte Carlo method. It is revealed that PSN solid solutions undergo a transition to the ferroelectric rhombohedral phase through an intermediate phase, existing in a narrow temperature range. PST solid solutions undergo a ferroelectric phase transition directly from the paraelectric cubic to the ferroelectric rhombohedral phase.

## 1. INTRODUCTION

Solid solutions of oxides with the perovskite structure have attracted the attention of the researchers for many decades due to their unusual phase diagrams and extraordinary electromechanical properties [1–3]. Among numerous ferroelectric materials, $PbSc_{0.5}Ta_{0.5}O_3$ (PST) and $PbSc_{0.5}Nd_{0.5}O_3$ (PSN) solid solutions are of particular interest. The physical properties and character of phase transitions in these compounds depend on the degree of ordering of scandium and tantalum (niobium) ions. Completely disordered PST and PSN solid solutions manifest relaxor properties with a diffuse ferroelectric phase transition, whereas ordered $Pb_2ScTaO_6$ and $Pb_2ScNbO_6$ compounds behave as conventional ferroelectrics.

The high-temperature phase of disordered PST and PSN solid solutions has the $Pm3m$ symmetry (perovskite structure), while ordered solid solutions have the $Fm3m$ symmetry (elpasolite structure). With a decrease in temperature, both ordered and disordered solid solutions undergo a ferroelectric phase transition to the rhombohedral phase. The symmetry of the low-temperature phase of PSN is $R3m$. The symmetry of the low-temperature rhombohedral phase of PST has not been finally determined [4]. The ferroelectric phase transition and electromechanical properties of these solid solutions have been experimentally investigated in detail (see, for example, [5] and references therein). An important feature of these compounds is their fairly

high (1500 K) temperatures of cationic ordering; thus, the degree of this ordering can be controlled by appropriate thermal conditions. As was shown in [6–8], disordered solid solutions contain ordered nanoregions. Their presence is confirmed by experimental investigations of the crystal lattice dynamics by the spectroscopic method [7, 8]. According to the symmetry, there are no active Raman modes in the high-temperature phase of disordered solid solutions; however, the investigations show that the spectra of ordered and disordered compounds are almost identical. As a result of the presence of ordered nanoregions, disordered solid solutions exhibit a more complicated pattern of lattice distortion during a ferroelectric phase transition in comparison with ordered PSN and PST. In this case, as was noted in [6, 9], not only the ferroelectric "soft" mode plays an important role during phase transition but also the antiferroelectric soft mode in PSN and the soft mode (due to octahedron rotation) in PST.

Calculations of the ferroelectric phase transition and physical properties within the local density functional method were performed mainly for PSN, using a model Hamiltonian and the local-mode approximation. A brief review of the results obtained with indication of the corresponding references can be found in Burton's paper [10].

In [11], the high-frequency permittivity, dynamic Born charges, and the frequency spectrum of lattice vibrations were calculated for ordered and disordered

**Table 1.** Eigenvectors of the ferroelectric mode, permittivities, and dynamic charges (in $e$ units) for disordered and ordered PSN and PST

| | | | Pb | $\langle$ScNb(Ta)$\rangle$ | $O_\perp$ | $O_\parallel$ |
|---|---|---|---|---|---|---|
| | | Disordered solid solutions (perovskite structure) | | | | |
| | $\varepsilon_\infty$ | | Pb | $\langle$ScNb(Ta)$\rangle$ | $O_\perp$ | $O_\parallel$ |
| $PbSc_{0.5}Nb_{0.5}O_3$ | 3.55 | $\xi$ | 0.76 | 0.21 | −0.42 | −0.14 |
| | | $Z_{dyn}$ | 2.69 | 5.16 | −1.89 | −4.19 |
| $PbSc_{0.5}Ta_{0.5}O_3$ | 3.32 | $\xi$ | 0.77 | 0.11 | −0.44 | −0.01 |
| | | $Z_{dyn}$ | 2.64 | 4.28 | 2.02 | 2.88 |
| | | Ordered solid solutions (elpasolite structure) | | | | |
| | | | Pb | Nb(Ta) | Sc | $O_\perp$ | $O_\parallel$ |
| $Pb_2ScNbO_6$ | 3.58 | $\xi$ | 0.53 | 0.07 | 0.27 | −0.29 | −0.11 |
| | | $Z_{dyn}$ | 2.71 | 5.93 | 4.19 | −1.80 | −4.17 |
| $Pb_2ScTaO_6$ | 3.32 | $\xi$ | 0.54 | 0.07 | 0.12 | −0.31 | 0.00 |
| | | $Z_{dyn}$ | 2.67 | 4.20 | 3.89 | 2.04 | 2.64 |

PSN and PST within the generalized Gordon–Kim model of an ionic crystal, taking into account the multipole polarizabilities. It was found for all the compounds under consideration that there is ferroelectric lattice instability in the symmetric cubic phase. The purpose of this study is to calculate (within the same model of an ionic crystal) the temperature of the ferroelectric phase transition and spontaneous polarization in ordered and disordered PSN and PST.

In Section 2, we report the model Hamiltonian describing the ferroelectric phase transition in completely disordered PSN and PST compounds with the perovskite structure and in cation-ordered Sc, Nb(Ta) solid solutions with the elpasolite structure. The explicit form of the model Hamiltonian for the perovskite structure was given in [12, 13]. Here, we report the explicit form of the Hamiltonian for the elpasolite structure. In Section 3, the parameters of the model Hamiltonians for PSN and PST with the perovskite and elpasolite structures are determined from calculations of the total energy of the phases distorted with respect to the eigenvectors of the ferroelectric mode. In Section 4, we discuss the results of the Monte Carlo calculation of the statistical properties of the compounds under consideration. Finally, the main results of this study are briefly formulated in Conclusions.

## 2. MODEL HAMILTONIAN IN THE LOCAL-MODE APPROXIMATION

To calculate the temperatures of the ferroelectric phase transition and the temperature dependence of spontaneous polarization, we will use the approach based on the local-mode approximation [12–14] to construct the effective Hamiltonian.

As was noted in Introduction, the lattice vibration frequencies for the compounds considered here were calculated in [11] and unstable ferroelectric modes were revealed in the oscillation spectrum. Table 1 contains the eigenvectors of unstable ferroelectric modes, high-frequency permittivities, and dynamic ion charges for the ordered and disordered PSN and PST cubic phases. It should be noted that, in the case of disordered solid solutions with the perovskite structure, all the calculations, of both the crystal lattice dynamics in [11] and the total energies of undistorted and distorted (with respect to the local-mode eigenvector) phases, reported below, were performed within the virtual-crystal approximation, i.e., for the Pb$\langle$B$\rangle$O$_3$ compound, where $\langle$B$\rangle$ is a virtual ion. It can be seen in Table 1 that, for all the compounds studied, lead ions have the largest displacements in the soft ferroelectric vibration mode. The Hamiltonian has the form

$$E_{tot} = E_{anhar}(\{\mathbf{S}_i\}) + E_{short}(\{\mathbf{S}_i\}, \{\mathbf{S}_j\}) + E_{dip}(\{\mathbf{S}_i\}, \{\mathbf{S}_j\}), \tag{1}$$

where $\mathbf{S}_i$ is the three-component (for both the perovskite and elpasolite structures) local soft mode in a cell, which is centered at Pb ions and is determined as $S^\alpha = u^\alpha \sum_i \xi_{i\alpha}$ ($u$ is the ion displacement amplitude and $\xi_{k\alpha}$ is the mode eigenvector from Table 1); the term

$$E_{anhar}(\{\mathbf{S}\}) = \sum_i (A\mathbf{S}_i^2 + B\mathbf{S}_i^4 + C(S_i^{x2}S_i^{y2} + S_i^{x2}S_i^{z2} + S_i^{y2}S_i^{z2})) \tag{2}$$
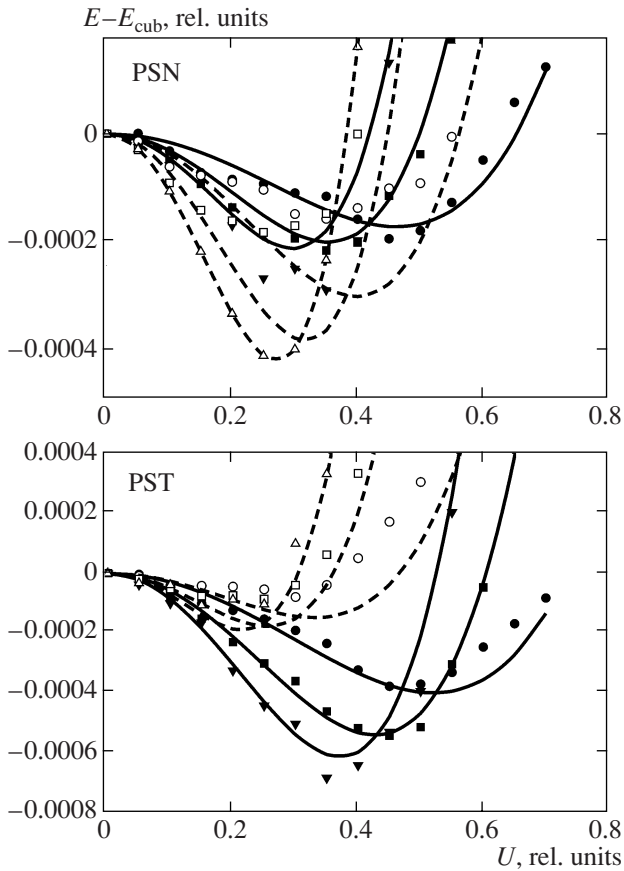
**Fig. 1.** Dependences of the total energy of PSN and PST on the local-mode amplitude. Open symbols and dotted lines correspond to disordered compounds; filled symbols and solid lines correspond to ordered ones. Circles, squares, and triangles show the displacements of one, two, and three local-mode components. The lines show the energies calculated according to (2) with the coefficients from Table 3.

is the anharmonic contribution to the local-mode energy within a cell; and the term

$$E_{\text{dip}}(\{\mathbf{S}_i\}, \{\mathbf{S}_j\}) = \frac{3(Z^*)^2}{\varepsilon_\infty + 2} \sum_{ij,\,\alpha\beta} Q_{ij}^{\alpha\beta} u_i^\alpha u_j^\beta \quad (3)$$

describes the long-range dipole–dipole interactions between local modes. Here, $Z^* = \sum_{\alpha k} Z_{\text{din}}^{\alpha k} \xi_{k\alpha}$ is the dynamic charge of the local mode with $\xi_{k\alpha}$ and $Z_{\text{din}}^{\alpha k}$ from Table 1 and $Q_{ij}^{\alpha\beta}$ are the structural constants, which depend on the lattice geometry and are calculated by the Ewald method. We should note here that the energy of long-range dipole–dipole interactions was calculated in [12, 13] using another expression:

$$E_{\text{dip}}(\{\mathbf{S}_i\}, \{\mathbf{S}_j\}) = \frac{(Z^*)^2}{\varepsilon_\infty} \sum_{ij,\,\alpha\beta} Q_{ij}^{\alpha\beta} u_i^\alpha u_j^\beta.$$

However, Kvyatkovskii showed [15] that long-range dipole–dipole interactions between crystal cells are determined from formula (3). Finally, the term

$$E_{\text{short}}(\{\mathbf{S}_i\}, \{\mathbf{S}_j\}) = \frac{1}{2} \sum_{i \neq j} \sum_{\alpha\beta} J_{ij,\,\alpha\beta} S_i^\alpha S_j^\beta \quad (4)$$

describes the short-range interaction between local modes within several coordination spheres. For the perovskite structure, the explicit form of $J_{ij,\,\alpha\beta}$ was given in [13], where the short-range interactions between local modes are taken into account within three coordination spheres. In the ordered PSN and PST solid solutions with the fcc elpasolite structure, the number of nearest neighbors is large; hence, for simplicity, we will restrict ourselves to consideration of short-range interactions within two coordination spheres. In this case, $J_{ij,\,\alpha\beta}$ for the first and second coordination spheres can be written, respectively, as

$$J_{ij,\,\alpha\beta} = (a_1 + \sqrt{2}(a_2 - a_1)|r_{ij,\,\alpha}|)\delta_{\alpha\beta} \\ + 2a_3(1 - \delta_{\alpha\beta})|r_{ij,\,\alpha}||r_{ij,\,\beta}| \quad (5a)$$

and

$$J_{ij,\,\alpha\beta} = (b_2 + (b_1 - b_2)|r_{ij,\,\alpha}|)\delta_{\alpha\beta}, \quad (5b)$$

where $\mathbf{r}_{ij} = \mathbf{R}_{ij}/|\mathbf{R}_{ij}|$ are the direction cosines.

## 3. DETERMINATION OF THE EFFECTIVE-HAMILTONIAN PARAMETERS

The parameters of the one-cell anharmonic potential, $B$ and $C$, were found from the dependences of the total energy of a crystal on the amplitudes of one, two, and three components of uniform displacements in a local mode. These dependences are shown in Fig. 1.

The parameters of short-range interactions between local modes in different cells were determined from the difference in the total energies of the cubic and distorted phases. In this case, the energies of the distorted structures were calculated with the ion-displacement amplitude corresponding to the energy minimum in the dependences shown in Fig. 1. For disordered solutions, we used the distorted structures reported in [13] and, respectively, the same designations for the parameters of short-range interactions. For ordered PSN and PST, a set of structures distorted with respect to the local-mode vector is shown in Fig. 2. The parameters of short-range interactions were determined from the system of equations whose right-hand side is the difference between the total energies of the crystal in the distorted and cubic phases, without anharmonic and dipole–dipole contributions. These systems of equations are listed in Table 2, which contains also the dipole contributions to the energy of distorted structures. The numerical values of the effective-Hamilto-

1. $\mathbf{q} = (0, 0, 0)$
$S_x = S_y = 0; S_z = 1$

2. $\mathbf{q} = (0, 0, 2\pi/a)$
$S_x = S_y = 0; S_z = 1$

3. $\mathbf{q} = (0, 0, 2\pi/a)$
$S_x = 1; S_y = S_z = 0$

4. $\mathbf{q} = (\pi/a, \pi/a, \pi/a)$
$S_x = S_y = S_z = 1$

5. $\mathbf{q} = (\pi/a, 0, 2\pi/a)$
$S_x = S_z = 0; S_y = 1$

6. $\mathbf{q} = (\pi/a, 0, 2\pi/a)$
$S_x = S_z = 1; S_y = 0$
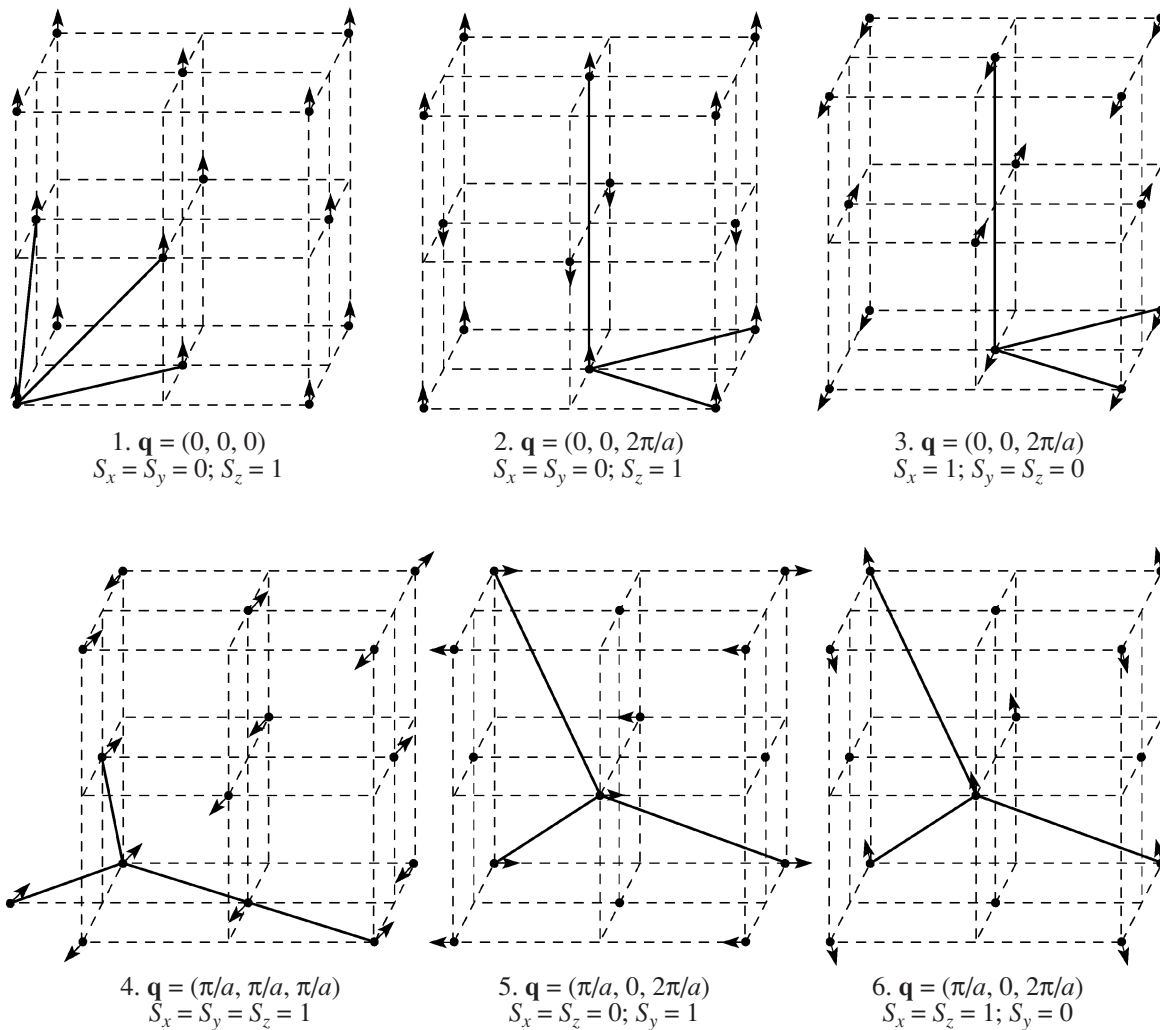
**Fig. 2.** Distorted structures used to calculate the effective-Hamiltonian coefficients for ordered solid solutions with the elpasolite structure. The arrows show the direction of the local-mode displacement at a site; the solid lines show the unit-cell vectors of the distorted structures.

nian parameters, describing the ferroelectric phase transitions in disordered and ordered PSN and PST, are listed in Table 3.

## 4. RESULTS OF THE CALCULATION OF STATISTICAL PROPERTIES AND THEIR DISCUSSION

The statistical mechanics of disordered and ordered solid solutions with the effective Hamiltonian (1) was investigated by the standard Monte Carlo method [16]. The calculation was performed for a $10 \times 10 \times 10$ simple cubic lattice (in the case of disordered solutions with the perovskite structure) and a $12 \times 12 \times 12$ fcc lattice (for ordered solutions) with periodic boundary conditions. To take into account the long-range dipole–dipole interactions in the Monte Carlo procedure, the structural constants $Q_{ij}^{\alpha\beta}$ were previously calculated by

the Ewald method and were not changed any more [13]. The Monte Carlo procedure was started from both high and low temperatures and with different initial configurations (both completely disordered, with $S^x = S^y = S^z = 0$ at all lattice sites, and completely ordered, with $S^x = S^y = S^z \neq 0$). The temperature step was 10–20 K. For each temperature, the first $4 \times 10^4$ Monte Carlo steps were used to prepare the equilibrium state of the system and were not involved in averaging of the thermodynamic values; averaging was performed over next $10^4$ steps. In the phase-transition range, the number of Monte Carlo steps was doubled. The Monte Carlo results for all the compounds under study are presented in Figs. 3–5 and Table 4. Figures 3 and 4 show the temperature dependences of the three components of the transition parameter and internal energy for disordered and ordered PSN and PST. It can be seen in Fig. 4 that one phase transition from the paraelectric cubic to the

**Table 2.** Energies of distorted structures (the expressions for the short-range energies of disordered compositions are taken from [13])

| | Disordered solid solutions | | | |
|---|---|---|---|---|
| | PSN | | PST | |
| | $E_{short}$, eV | $E_{dip}$, eV | $E_{short}$, eV | $E_{dip}$, eV |
| (a) $2j_1 + j_2 + 4j_3 + 2j_4 + 4j_6 + A$ | 106.8 | −111.3 | 74.3 | −77.5 |
| (b) $2j_1 - j_2 + 4j_3 + 2j_4 - 4j_6 + A$ | −201.1 | 257.5 | −110.1 | 179.2 |
| (c) $j_2 - 2j_4 - 4j_6 + A$ | 135.5 | −128.7 | 94.9 | −89.6 |
| (d) $-2j_1 + j_2 - 4j_3 + 2j_4 + 4j_6 + A$ | 151.1 | −142.3 | 108.2 | −99.0 |
| (e) $-j_2 - 2j_4 + 4j_6 + A$ | −23.2 | 71.1 | 53.7 | 49.5 |
| (f) $-2j_1 - j_2 + 4j_3 + 2j_4 - 4j_6 + A$ | 38.8 | 0.0 | 39.7 | 0.0 |
| (g) $j_1 - 2j_5 - 4j_7 + A/2$ | −74.2 | 77.9 | −46.6 | 54.2 |
| | Ordered solid solutions | | | |
| | PSN | | PST | |
| | $E_{short}$, eV | $E_{dip}$, eV | $E_{short}$, eV | $E_{dip}$, eV |
| $E_{\Gamma, z(x, y)} = 2a_1 + 4a_2 + b_1 + 2b_2 + A$ | 424.7 | −436.0 | 289.3 | −308.4 |
| $E_{Z, z} = 2a_1 - 4a_2 + b_1 + 2b_2 + A$ | −270.1 | 451.1 | −195.8 | 319.1 |
| $E_{Z, x} = -2a_1 + b_1 + 2b_2 + A$ | 260.7 | −225.6 | 189.9 | −159.5 |
| $E_L = -12a_3 - 3b_1 - 6b_2 + 3A$ | −1511.0 | 2257.9 | −733.1 | 1597.0 |
| $E_{W, y} = -a_2 + b_1/2 + A/2$ | 1.9 | 41.0 | 3.1 | 29.0 |
| $E_{W, xz} = -a_1 - a_2 + b_2 + A$ | 118.9 | −41.0 | 93.8 | −29.0 |

ferroelectric rhombohedral phase with nonzero (and approximately equal) values of all three components of the order parameter occurs in ordered and disordered $PbSc_{0.5}Ta_{0.5}O_3$ solid solutions. In the case of both

**Table 3.** Parameters of the model Hamiltonian (in eV)

| | Disordered solid solutions | | | Ordered solid solutions | |
|---|---|---|---|---|---|
| | PSN | PST | | PSN | PST |
| $j_1$ | −35.48 | −22.96 | $a_1$ | −44.68 | −34.93 |
| $j_2$ | 92.24 | 41.77 | $a_2$ | 87.24 | 61.06 |
| $j_3$ | 12.22 | 7.26 | $a_3$ | 152.17 | 101.79 |
| $j_4$ | −8.05 | −11.61 | $b_1$ | 14.76 | 3.66 |
| $j_5$ | 24.17 | 16.45 | $b_2$ | −14.52 | −13.02 |
| $j_6$ | 32.09 | 5.32 | | | |
| $j_7$ | 1.61 | 2.66 | | | |
| $A$ | 40 | 51 | $A$ | 180 | 137 |
| $B$ | 1176 | 1193 | $B$ | 5880 | 8343 |
| $C$ | 1350 | 1602 | $C$ | 8411 | 7970 |
| $z$ | 5.28 | 4.31 | $z$ | 7.41 | 6.08 |
| $\varepsilon_\infty$ | 3.55 | 3.32 | $\varepsilon_\infty$ | 3.58 | 3.32 |

ordered and disordered $PbSc_{0.5}Nd_{0.5}O_3$ compounds (Fig. 3), according to the Monte Carlo data, the phase transition to the rhombohedral phase occurs through an intermediate phase (orthorhombic or monoclinic) with two nonzero components of the three-component order parameter. The temperature range of existence of this intermediate phase is several tens of kelvins. It is difficult to find the transition temperatures from the temperature dependences of the order parameter and internal energy (due to the presence of tails in the dependences of the order parameter, which are related to the finite sizes of the system, and almost smooth dependence of the internal energy). We determined the phase-transition temperatures from the temperature dependences of the individual contributions, $E_{anharm}$, $E_{short}$, and $E_{dip}$, to the internal energy of the system, whose nonmonotonic dependence is more pronounced. These dependences, along with that of the internal energy, are shown in Fig. 3. It can be seen that, in the case of PST, there is an inflection at the point corresponding to the falloff temperature in the dependences of the transition parameter. At the same time, for POSITION, the dependences of the individual contribution to the energy contain two inflection points at the temperatures corresponding to two-step decrease: first in one component and then in the two remaining components of the transition param-

**Fig. 3.** Temperature dependences of the local-mode amplitude (a, b) and energies (c, d) for ordered (a, c) and disordered (b, d) PSN. In panels (a, b), circles, squares, and triangles indicate, respectively, the largest, intermediate, and smallest local-mode components. The vertical dashed lines pass through the inflection points in the energy dependences.

eter. The found values of the ferroelectric phase transition temperatures, along with the experimental values, are listed in Table 4. According to the data of Table 4, the results of the calculation of the ferroelectric phase transition from the cubic to the rhombohedral phase in PST qualitatively correctly describe the experimental situation, specifically: in an ordered compound, transition occurs at a higher temperature in comparison with a disordered one. The agreement between the calculated and experimental values of the transition temperature can be considered as satisfactory. For PSN, the results of the calculation are similar to those for PST but are inconsistent with the experimental data, according to which the ferroelectric transition to the rhombohedral phase in an ordered compound occurs at a lower temperature in comparison with a disordered one. Moreover, according to the Monte Carlo data, there are two phase transitions in PSN; i.e., the transition from the cubic to the rhombohedral phase occurs through an intermediate phase with two (nonzero) components of spontaneous polarization, and the temperature range of

existence of this intermediate phase is several tens of kelvins. To the best of our knowledge, there are no experimental data on the existence of such a phase in PSN. The spontaneous polarization $P_s$ in the ferroelectric phase is defined as

$$P_s = Z^* \langle \sqrt{u_x^2 + u_y^2 + u_z^2} \rangle, \qquad (6)$$

where $Z^*$ is the dynamic charge of the ferroelectric mode, determined above, and averaging is over the last $10^4$ Monte Carlo steps. Figure 5 shows the temperature dependence of $P_s$ for all four compounds considered here and Table 4 contains the values of saturation polarization, along with the experimental data. Table 4 gives also the calculated and experimental values of maximum displacements of ions in the ferroelectric phase
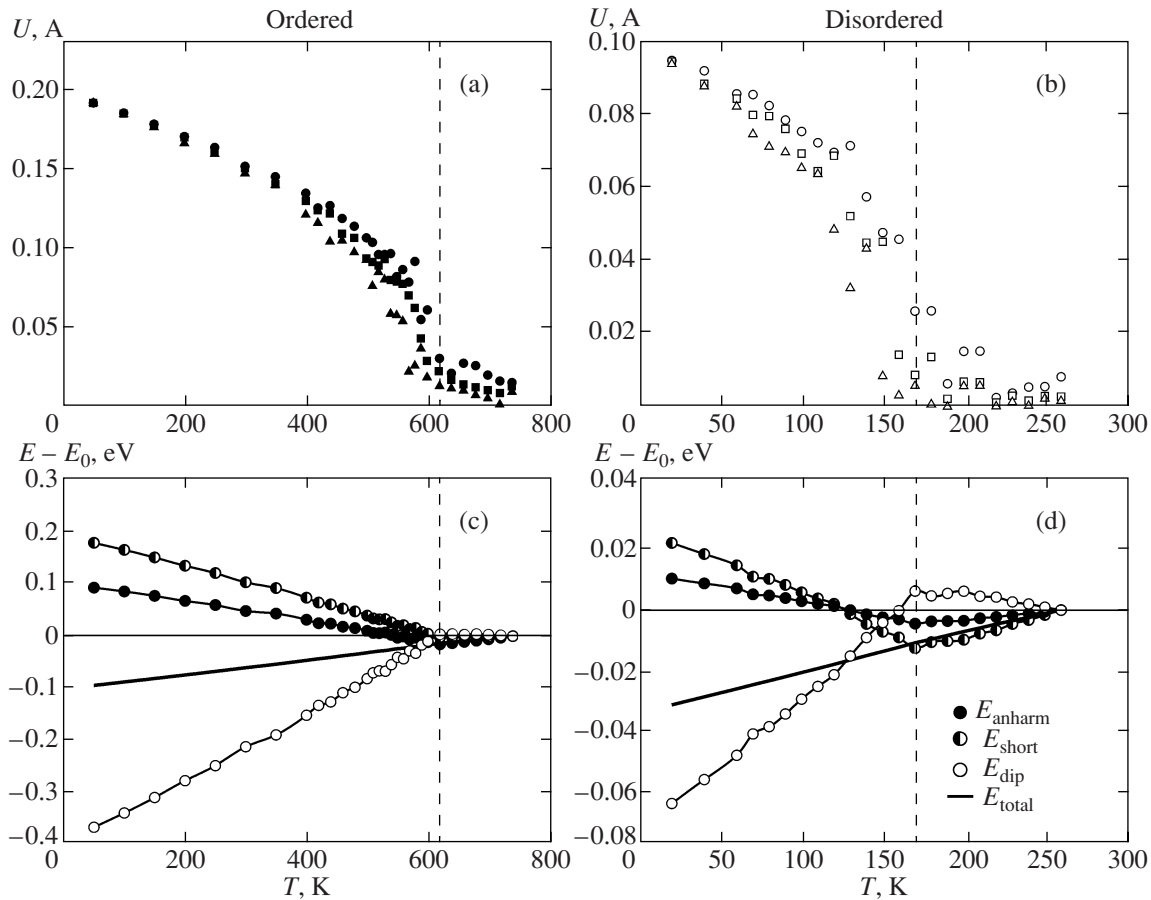
**Fig. 4.** The same as in Fig. 3 but for PST.

from the equilibrium positions of the cubic phase. One can see good agreement between the calculated and experimental values of both the spontaneous polarization and ion displacements.
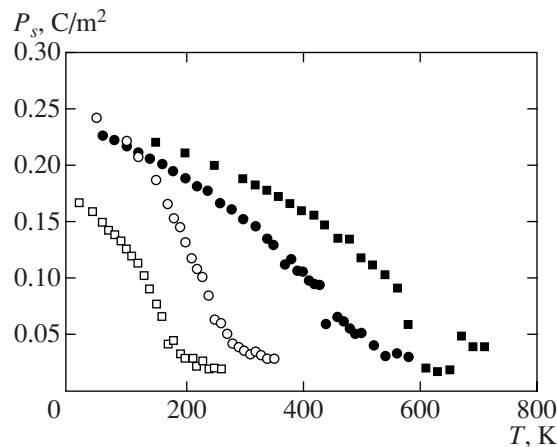


**Fig. 5.** Calculated temperature dependences of the spontaneous polarization for disordered (open symbols) and ordered (filled symbols) PSN (squares) and PST (circles).

## 5. CONCLUSIONS

In this study, we calculated the ferroelectric-phase transition temperatures, spontaneous polarization, and ion displacements in the ferroelectric phase for $PbSc_{0.5}Ta_{0.5}O_3$) and $PbSc_{0.5}Nd_{0.5}O_3$ solid solutions by the effective-Hamiltonian method. The calculation was performed within the local-mode approximation for polar lattice vibrations, applying the Monte Carlo procedure to determine the statistical properties. The parameters of the effective Hamiltonian were derived from the ab initio calculation of the total energy of the crystal within the model of an ionic crystal, taking into account the dipole and quadrupole polarizabilities of ions. We obtained the following results.

(i) The calculated values of the spontaneous polarization and ion displacements in the ferroelectric phase are in good agreement with the experimental data for all four compounds under consideration (ordered and disordered PSN and PST).

(ii) For ordered PSN and PST, the calculated ferroelectric-transition temperature $T_c$ exceed the experimental values by factors of 1.5 and 2.0, respectively. For disordered solutions, the calculated $T_c$, vice versa,

**Table 4.** Phase-transition temperatures, spontaneous polarization, and ion displacements in the [111] direction for disordered and ordered PSN and PST (the last two columns give relative displacements of the corresponding ions; the experimental data are taken from [17])

| | | Disordered solid solutions (perovskite structure) | | | | | | | |

| | | \multicolumn{2}{} | | \multicolumn{5}{Ion displacements, Å} | | | | |
|---|---|---|---|---|---|---|---|---|---|
| | | $T_c$, K | | $P_s$, C/m$^2$ | Pb | $\langle ScNb(Ta)\rangle$ | O | $\delta_{Pb-O}$ | $\delta_{\langle B\rangle-O}$ |
| PbSc$_{0.5}$Nb$_{0.5}$O$_3$ | calculation | 220 | 250 | 0.26 | 0.17 | 0.05 | −0.09 | 0.26 | 0.14 |
| | experiment | – | 380 | – | – | – | – | 0.39 | 0.16 |
| PbSc$_{0.5}$Ta$_{0.5}$O$_3$ | calculation | 170 | | 0.17 | 0.14 | 0.02 | −0.06 | 0.20 | 0.08 |
| | experiment | 275 | | 0.33 | – | – | – | – | – |

Ordered solid solutions (elpasolite structure)

| | | $T_c$, K | | $P_s$, C/m$^2$ | Pb | Nb(Ta) | Sc | O | $\delta_{Pb-O}$ | $\delta_{\langle Sc\rangle-O}$ |
|---|---|---|---|---|---|---|---|---|---|---|
| Pb$_2$ScNbO$_6$ | calculation | 400 | 490 | 0.24 | 0.14 | 0.02 | 0.07 | −0.09 | 0.23 | 0.16 |
| | experiment | – | 350 | 0.26 | – | – | – | – | 0.36 | 0.14 |
| Pb$_2$ScTaO$_6$ | calculation | 610 | | 0.24 | 0.17 | 0.02 | 0.04 | −0.08 | 0.25 | 0.12 |
| | experiment | 300 | | – | – | 0.0 | 0.0 | – | – | – |

are smaller than the experimental values by 130 and 75 K, respectively.

(iii) For the PSN solid solution, the Monte Carlo data indicate a sequence of two ferroelectric phase transitions: paraelectric cubic phase ⟶ ferroelectric monoclinic (or orthorhombic) phase with two polarization components ⟶ ferroelectric rhombohedral phase with three (nonzero) polarization components. The intermediate phase exists in a fairly narrow temperature range (of about 50 K). According to the experimental data, this compound is characterized by a single-phase transition from the cubic to the rhombohedral phase.

## REFERENCES

1. L. E. Cross, Ferroelectrics **76**, 241 (1987).

2. N. Takesue, Y. Fujii, M. Ichihara, and H. Chen, Phys. Rev. Lett. **82**, 3709 (1999).

3. C. Perrin, N. Menguy, O. Bidault, et al., J. Phys.: Condens. Matter **13**, 10231 (2001).

4. P. M. Woodward and K. Z. Baba-Kishi, J. Appl. Crystallogr. **35**, 233 (2002).

5. V. A. Isupov, Ferroelectrics **289**, 131 (2003).

6. V. V. Laguta, M. D. Glinchuk, I. P. Bykov, et al., Phys. Rev. B: Condens. Matter **69**, 054103 (2004).

7. I. G. Siny, S. G. Lushnikov, and R. S. Katiyar, Ferroelectrics **231**, 115 (1999).

8. E. A. Rogacheva, Physica B (Amsterdam) **291**, 359 (2000).

9. W. Dmowski, M. K. Akbas, P. K. Davies, and T. Egami, J. Phys. Chem. Solids **61**, 229 (2000).

10. B. P. Burton, E. Cockayne, S. Tinte, and U. V. Waghmare, Phase Transitions **79**, 91 (2006).

11. V. I. Zinenko, N. G. Zamkova, E. G. Maksimov, and S. N. Sofronova, Zh. Éksp. Teor. Fiz. **132** (3), 702 (2007) [JETP **105** (3), 617 (2007)].

12. U. V. Waghmare and K. M. Rabe, Phys. Rev. B: Condens. Matter **55**, 6161 (1997).

13. W. Zhong and D. Vanderbilt, Phys. Rev. B: Condens. Matter **52**, 6301 (1995).

14. K. M. Rabe and J. D. Jannopoulos, Phys. Rev. B: Condens. Matter **36**, 6631 (1987).

15. O. E. Kvyatkovskii, Ferroelectrics **153**, 201 (1994); O. E. Kvyatkovskiĭ, Kristallografiya **49** (1), 8 (2004) [Crystallogr. Rep. **49** (1), 4 (2004)].

16. N. Metropolis, A. W. Rosenbluth, M. N. Rosenbluth, et al., Chem. Phys. **21**, 1087 (1953).

17. C. Malibert, B. Dkhil, J. M. Kiat, et al., J. Phys.: Condens. Matter **9**, 7485 (1997).

*Translated by Yu. Sin'kov*